

A Fast Least-Squares Arrival Time Estimator for Scintillation Pulses

Nicholas Petrick*, Alfred O. Hero III, Neal H. Clinthorne and W. Leslie Rogers
The University of Michigan, Department of Electrical Engineering
and Computer Science and Division of Nuclear Medicine.
Ann Arbor, MI 48109-0552

ABSTRACT

The true weighted least-squares (WLS) arrival time estimator for scintillation pulse detection was previously found to out-perform conventional arrival time estimators such as leading-edge and constant-fraction timers, but has limited applications because of its complexity. A new diagonalized version of the weighted least-squares (DWLS) estimator has been developed which, like the true WLS, incorporates the statistical properties of the scintillation detector. The new DWLS reduces estimator complexity at the expense of fundamental timing resolution. The advantage of the DWLS implementation is that only scalar multiplications and additions are needed instead of the matrix operations used in the true WLS. It also preserves the true WLS's ability to effectively separate piled-up pulses. The DWLS estimator has been applied to pulses which approximate the response of BGO and NaI(Tl) scintillation detectors. The timing resolution obtained with the DWLS estimator is then compared to conventional analog timers along with the Cramér-Rao lower bound on achievable timing error. The DWLS out-performs the conventional arrival time estimators but does not provide optimal performance compared to the lower bound; however, it is more robust than the true WLS estimator.

I. INTRODUCTION

In order to improve the timing resolution in scintillation pulse detection, a weighted least-squares (WLS) arrival time estimator was developed by Petrick *et. al.* [1]. This estimator incorporates the first-order and second-order statistics of the detection signal into the estimator structure, unlike the common leading-edge [2] and constant-fraction [3] timers. The general form for the single-pulse WLS timing estimator was derived in [1] and is given as

$$\tau_{wls}^d = \arg \min_{\tau} (\mathbf{X} - \hat{\boldsymbol{\mu}}(\tau))^T \hat{\mathbf{K}}^{-1}(\tau) (\mathbf{X} - \hat{\boldsymbol{\mu}}(\tau)), \quad (1)$$

where

$$\hat{\boldsymbol{\mu}}(\tau) = E\{\mathbf{X}(\tau)\} \quad (2)$$

$$\hat{\mathbf{K}}(\tau) = E\{(\mathbf{X}(\tau) - \hat{\boldsymbol{\mu}})(\mathbf{X}(\tau) - \hat{\boldsymbol{\mu}})^T\}, \quad (3)$$

*This work is supported by the National Cancer Institute, DHHS, under grant CA46622.

are the estimated mean and covariance function of the detected signal respectively. The general WLS structure was then expanded in [1] to the detection of a pair of piled-up optical pulses and is given as

$$\tau_{wls}^d = \arg \min_{\tau_1, \tau_2} [(\mathbf{X} - \hat{\boldsymbol{\mu}}(\tau_1) - \hat{\boldsymbol{\mu}}(\tau_2))^T \cdot (\hat{\mathbf{K}}(\tau_1) + \hat{\mathbf{K}}(\tau_2))^{-1} \cdot (\mathbf{X} - \hat{\boldsymbol{\mu}}(\tau_1) - \hat{\boldsymbol{\mu}}(\tau_2))], \quad (4)$$

where $\hat{\boldsymbol{\mu}}(\tau_i)$ and $\hat{\mathbf{K}}(\tau_i)$ correspond to the estimated single-pulse mean and covariance of Eqs. (2) and (3). The WLS estimator was found to significantly out-perform both the leading-edge and constant-fraction timers for simulated BGO and NaI(Tl) scintillator pulses [4]. The WLS structure also provided the ability to accurately detect multiple overlapping pulses. This full WLS implementation has found limited application in real-time systems because of its computational complexity. In the single-pulse implementation of Eq. (1), $\hat{\mathbf{K}}^{-1}(\tau)$ can be precomputed but two matrix multiplications must still be performed for each time step. This either restricts the sampling rate of the data collection or relegates the estimator to off-line applications. The problem is compounded in the double-pulse case where, along with the matrix multiplications, a matrix inversion must also be performed for each time step.

In this paper, we propose a variation on the full WLS arrival time estimator. This new estimator, denoted the diagonalized weighted least-squares (DWLS) arrival time estimator, is a simplified version of the WLS algorithm which still incorporates the first-order and second-order moments of the scintillation signal. The DWLS estimator was applied to scintillator-type optical pulses having a fast rise time and a longer exponential decay in an analogous fashion to [4]. Each of the optical pulses produce between 100 and 1000 photo-electrons in the PM tube's photo cathode, which is a range consistent with the optical signals produced by BGO and NaI(Tl) scintillation crystals when stimulated by 511 KeV gamma rays.

II. DIAGONALIZED WEIGHTED LEAST SQUARES TIMING ESTIMATOR

The diagonalized weighted least-squares (DWLS) arrival time estimator was developed as a simplified implementation of the WLS algorithm by zeroing all off-diagonal terms in the covariance matrix. It has the form of a WLS algorithm where the weighting is given by the inverse of the diagonal elements of the covariance function, K . The DWLS estimator can therefore be written as

$$\tau_{dwls}^d = \arg \min_{\tau} \left\{ \sum_{i=1}^{n-1} \frac{1}{[K(\tau)]_{i,i}} (x_i - \mu_i(\tau))^2 \right\}, \quad (5)$$

for the single-pulse case, and is extended to piled-up pulses by minimizing over all the arrival times. This leads to a double pulse DWLS estimator given by

$$\tau_{dwls}^d = \arg \min_{\tau_1, \tau_2} \left\{ \sum_{i=0}^{n-1} \frac{(x_i - \mu_i(\tau_1) - \mu_i(\tau_2))^2}{[K(\tau_1)]_{i,i} + [K(\tau_2)]_{i,i}} \right\}. \quad (6)$$

The diagonalized implementation becomes obvious upon examination of the multiple-photon covariance estimate, $K(\tau)$. Fig. 1 depicts the estimated covariance matrix for single optical pulses comprised of approximately 500 photons. This figure illustrates that for multiple photon pulses the off-diagonal terms are much smaller than the terms along the diagonal. In fact the width of the covariance is of the order of the single-electron response (SER) time width indicating that the correlation is due to the PM tube and not the optical source. Therefore, if the optical pulse width is large compared to the duration of the SER the covariance will be dominated by its diagonal elements.

III. CRAMÉR-RAO LOWER BOUND ON TIMING ERROR

In order to compare the WLS estimator's timing performance with the optimal minimum mean-squared error estimator, the Cramér-Rao (CR) lower bound over a range of large photo-electron intensities was introduced in [4]. The general form for the multi-dimensional covariance matrix for unbiased estimator errors $\hat{\tau} - \tau := [\hat{\tau}_1(\mathbf{X}) - \tau_1, \hat{\tau}_2(\mathbf{X}) - \tau_2]^T$ is given by

$$E \{ (\hat{\tau} - \tau)(\hat{\tau} - \tau)^T \} \geq J^{-1}, \quad (7)$$

where J is the Fisher information matrix [6]. The elements of J can be written as

$$[J]_{i,j} = -E \left\{ \frac{\partial^2 \ln p(\mathbf{X}|\tau_1, \tau_2)}{\partial \tau_i \partial \tau_j} \right\}, \quad (8)$$

and the CR bound on the variance of unbiased estimators for one of the arrival times, τ_i , is

$$E \{ (\tau_i - \hat{\tau}_i(\mathbf{X}))^2 \} \geq [J^{-1}]_{i,i}, \quad (9)$$

where $[J^{-1}]_{i,i}$ is the i, i^{th} element of the inverse Fisher information matrix J^{-1} [6].

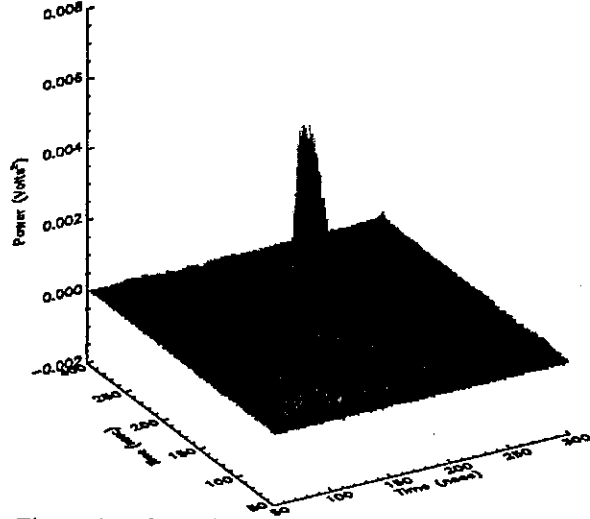


Figure 1: The estimated covariance from single optical pulses comprised of approximately 500 photons each.

Using the assumption that the detector response becomes Gaussian as the number of photo-electrons increases, it is possible to develop an expression for the high intensity CR lower bound based solely on the mean and covariance of the detector responses. The CR bound for single optical pulse simply reduces to

$$\text{CR Bound} = \left[\frac{d\mu(\tau)^T}{d\tau} K^{-1}(\tau) \frac{d\mu(\tau)}{d\tau} - \frac{1}{2} \sum_{i=1}^n \sum_{j=1}^n \frac{d^2 [K^{-1}(\tau)]_{i,j}}{d\tau^2} [K(\tau)]_{i,j} \right]^{-1}, \quad (10)$$

where $\mu(\tau)$ and $K(\tau)$ correspond to the mean and covariance of the detector response. The double-pulse CR has the form

$$\text{CR Bound} = \sqrt{[J^{-1}]_{1,1} + [J^{-1}]_{2,2}}, \quad (11)$$

where

$$[J]_{i,j} = \frac{1}{2} \frac{\partial \mu^T}{\partial \tau_i} K^{-1} \frac{\partial \mu}{\partial \tau_j} + \frac{1}{2} \frac{\partial \mu^T}{\partial \tau_j} K^{-1} \frac{\partial \mu}{\partial \tau_i} - \frac{1}{2} \sum_{l=1}^n \sum_{m=1}^n \frac{\partial^2 [K^{-1}]_{l,m}}{\partial \tau_i \partial \tau_j} [K]_{l,m}. \quad (12)$$

The parameters μ and K in Eq. (14) correspond to the double-pulse mean and covariance function, and were approximated using

$$\mu(\tau_1, \tau_2) = \hat{\mu}(\tau_1) + \hat{\mu}(\tau_2) \quad \text{and} \quad (13)$$

$$K(\tau_1, \tau_2) = \hat{K}(\tau_1) + \hat{K}(\tau_2). \quad (14)$$

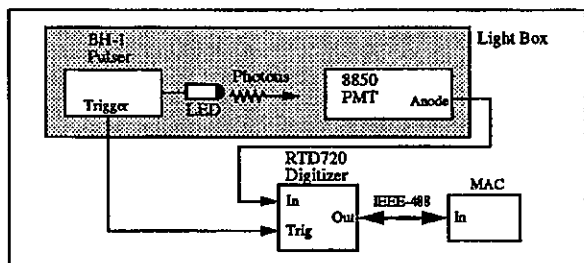


Figure 2: The experimental apparatus used to digitize the Burle 8850 PM tube's response to single optical pulses. Note, the input pulses were created using a Berkeley Nucleonics BH-1 tail-pulse generator and the output was digitized using a Tektronix RTD720 real-time digitizer.

IV. MATERIALS AND METHODS

The DWLS estimator was applied to the digitized output signal produced by a Burle 8850 PM tube. The experimental apparatus for digitizing the Burle 8850 PM tube's response to single optical pulses is depicted in Fig. 2. The single optical pulses were created by a pulsed LED and contained between 100 and 1000 photo-electrons per pulse. Fig. 3 show a typical optical intensity profile produced by the pulser and a light emitting diode. This pulse has an bi-exponential shape with a 20 ns rise and 50 ns decay time measured between 10% and 90% of the mean signal peak.

Three different sets of PM tube responses were digitized and stored using the apparatus of Fig. 2. The different sets of responses correspond to average optical intensities of 100, 500 and 1000 photo-electrons per optical pulse. In this study, over 2500 individual PM tube responses were digitized and stored for each optical intensity.

To evaluate the single-pulse diagonal WLS estimator, the mean and covariance matrices were estimated for each of the 100, 500 and 1000 photo-electron optical intensities using 2092 of the digitized responses. The estimated mean, $\hat{\mu}(\tau)$, and the diagonal terms in the estimated covariance, $\hat{K}(\tau)$, were then used in the application of the WLS estimator of Eq. (5). This estimator along with the full WLS estimator of Eq. (1) were applied to a set of 523 PM tube responses for each optical intensity and the results were compared to each other and to the Cramér-Rao lower bound for achievable timing error.

Pairs of piled-up PM tube responses were created with approximately 50% pulse overlap by combining 2 sets of digitized detector responses giving the typical intensity profile depicted in Fig. 4 with pulse separation $\tau_2 - \tau_1$. The estimated single-pulse mean and the diagonal terms of the estimated covariance were again used in the implementation of the double-pulse DWLS estimator of Eq. (6). In this case, the single-pulse mean, $\hat{\mu}$, and covariance, \hat{K} , were delayed by the two arrival time τ_1 and τ_2 . The delayed versions were then added to their counterparts to create the double-pulse mean and covariance. The double-pulse DWLS estimator was applied to a set of 523 double-

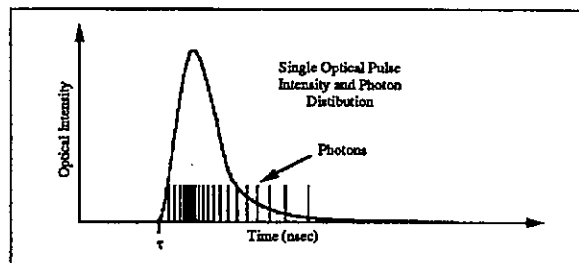


Figure 3: The exponentially shaped optical intensity and photo-electron distribution used to stimulate the Burle 8850 PM tube. The intensity has 20 ns rise and 50 ns decay components.

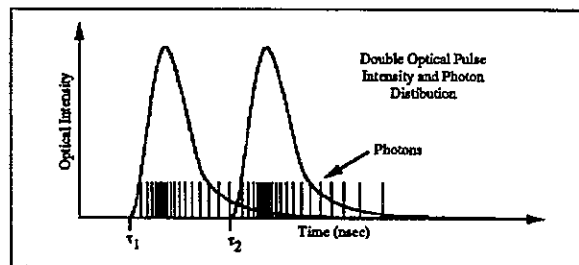


Figure 4: The exponentially shaped optical intensity and photo-electron distribution for a pair of overlapping optical pulses. Each of the single-pulse intensities has 20 ns rise and 50 ns decay component.

pulse PM tube responses and compared with the full WLS estimator and the CR lower bound on achievable timing performance.

The performance of the estimators were compared using the standard deviation (SD), $\sqrt{E\{(\hat{\tau}_i - E(\hat{\tau}_i))^2\}}$, of the arrival time estimates.

For a complete description of the digitization of the optical pulses and the implementation of both the full WLS and diagonalized WLS estimators refer to Refs. [4] and [5].

V. RESULTS AND DISCUSSION

The single-pulse DWLS estimator along with the full WLS estimator were applied to the digitized time histories. The resulting timing resolution for the 100, 500 and 1000 photo-electron optical pulse is given in Table 1 along with the measured leading-edge and constant-fraction resolutions. This table also includes the minimum achievable timing error given by the Cramér-Rao lower bound.

The DWLS estimator out-performs the analog leading-edge and constant-fraction timers when the optical intensity is low (*i.e.* the 100 photo-electron case) but these estimators are comparable for the large photo-electron intensities. This is not the case with the full WLS implementation where it maintains an advantage in the high intensity regime as well. None of the estimators approach the fundamental limit of the Cramér-Rao bound in this

Photons per Pulse	LE Error (ns)	CF Error (ns)	WLS Error (ns)	DWLS Error (ns)	CR Bound (ns)
100	3.03	2.96	1.99	2.36	0.117
500	1.98	1.92	1.40	1.87	0.109
1000	1.67	1.68	0.36	1.50	0.089

Table 1: The performance of the leading-edge (LE), constant-fraction (CF), WLS and DWLS arrival time estimators for the detection of single gamma rays where the optical pulses have 20 ns rises and 50 ns decays. This table also includes the Cramér-Rao (CR) lower bound on achievable timing error where the timing error is the standard deviation of the estimated arrival times.

Photons per Pulse	Overlap	DWLS Error (ns)	WLS Error (ns)	CR Bound (ns)
100	48.9%	4.02	5.71	0.297
500	50.9%	3.08	3.61	0.269
1000	50.7%	2.40	1.44	0.228

Table 2: The performance of the DWLS and the true WLS arrival time estimator for the detection of pairs of gamma rays where the optical pulses again have 20 ns rise times, 50 ns decays and overlap by 50%. This table also includes the double-pulse Cramér-Rao (CR) lower bound on timing error where the timing error is the standard deviation of the estimated arrival times.

implementation. The large error associated with the WLS estimator is probably due to the estimation errors in the off-diagonal terms of the covariance matrix [4].

The double-pulse timing resolution for the diagonalized and full WLS implementation is given in Table 2 along with the corresponding Cramér-Rao lower bounds.

These results indicate a different trend. The diagonalized estimator out-performs the full WLS implementation. This should not be the case if we have accurate measurements for the double-pulse mean, $\mu(\tau_1, \tau_2)$, and covariance matrix, $K(\tau_1, \tau_2)$. In the full WLS implementation we use the single-pulse covariance in the double-pulse implementation. A problem again arises with the off-diagonal terms in this covariance matrix. The off-diagonal terms in this matrix are much smaller than in the single-pulse case making them more difficult to estimate. The results of Table 2 indicate that we are not accurately estimating these off-diagonal terms, leading to the DWLS estimator out-performing the full WLS implementation. Table 3 summarizes the WLS error found when a matched covariance matrix is used in the estimator structure. From this table, we see that the full WLS implementation does indeed approach the Cramér-Rao bound while there is only slight improvement with the diagonalized version.

VI. CONCLUSION

These results indicate that the DWLS arrival time esti-

Photons per Pulse	Overlap	DWLS Error (ns)	WLS Error (ns)	CR Bound (ns)
500	50.9%	3.04	0.53	0.269

Table 3: The performance of the DWLS and the true WLS arrival time estimator using the matched covariance function, $K_{opt}(\tau)$, for the detection of pairs of gamma rays where the optical pulses again have 20 ns rise times, 50 ns decays and overlap by 50%. This table again include the double-pulse Cramér-Rao (CR) lower bound on timing error where the timing error is the standard deviation of the estimated arrival times.

imator can be used to approximate an optimal arrival time estimator and provides improved timing resolution over leading-edge and constant-fraction timers. The DWLS estimator structure is simply one of weighting and summing the output signal from a PM tube. This structure opens the possibility for a hardware implementation which would allow the estimator to be applied in real-time applications. A real-time implementation of this DWLS estimator would provide improved performance over leading-edge and constant-fraction timers when the detector produces a significant number of piled-up optical pulses, but would only provide small improvements for isolated optical pulses.

REFERENCES

- [1] N. Petrick, A.O. Hero, N.H. Clinthorne and W.L. Rogers, "Least Squares Arrival Time Estimators for Photons Detected using a Photomultiplier Tube," *IEEE Transactions on Nuclear Science*, **NS-39**(4): pp. 738-741, August 1992.
- [2] M.A. El-Wahab and M.A. El-Salam, "Timing Resolution in Leading Edge and Crossover Timing," *Nuclear Instruments and Methods*, **78**: pp. 325-327, 1970.
- [3] M.A. El-Wahab, A. El-Arabi and M.H. Battawi, "Constant Fraction Timing with Scintillation Detectors," *IEEE Transactions on Nuclear Science*, **NS-36**(1): pp. 401-406, February 1989.
- [4] N. Petrick, A.O. Hero, N.H. Clinthorne, W.L. Rogers and J. M. Slosar, "Least Squares Arrival Time Estimators for Single and Piled Up Scintillation Pulses," *IEEE Transactions on Nuclear Science*, **NS-40**(4): pp. 1026-1030, August 1993.
- [5] N. Petrick, *Optimal Arrival Time Estimators for Electromagnetic Radiation Detectors*, Ph.D. Dissertation, University of Michigan, Ann Arbor, MI, 1992.
- [6] Van Trees, H. L., *Detection Estimation and Modulation Theory: Part I*, New York: John Wiley and Sons, 1968.